Hindawi Publishing Corporation
Journal of Electrical and Computer Engineering
Volume 2014, Article ID 176560, 5 pages
http://dx.doi.org/10.1155/2014/176560

Research Article

Design of Dual-Band Bandpass Filter Using Dual-Mode Defected Stub Loaded Resonator

Dechang Huang[1] and Zhaodi Huang[2]

[1] *School of Information Engineering, East China Jiaotong University, Nanchang 330013, China*
[2] *School of Electrical and Electronic Engineering, East China Jiaotong University, Nanchang 330013, China*

Correspondence should be addressed to Dechang Huang; huangdechang2006@126.com

Received 1 May 2014; Revised 20 June 2014; Accepted 23 June 2014; Published 21 July 2014

Academic Editor: John N. Sahalos

A novel approach for designing a dual-band bandpass filter (BPF) using defected stub loaded resonator (DSLR) is presented in this paper. The proposed DSLR consists of two fundamental resonant modes and some resonant characteristics have been investigated by EM software of *Ansoft HFSS*. Then, based on two coupled DSLRs, a dual-band response BPF that operates at 2.4 GHz and 3.5 GHz is designed and implemented for WLAN and WIMAX application. The first passband is constructed by two lower frequencies of the coupled DSLRs and the second passband is produced by two higher ones; the coupling scheme of them is also given. Finally, the dual-band BPF is fabricated and measured; a good agreement between simulation and measurement is obtained, which verifies the validity of the design methodology.

1. Introduction

Modern development in wireless communication systems has led to an increasing demand for dual-band microwave passive devices. As a key circuit block in dual-band wireless communication, such as for both global system for mobile communications (GSM) and wireless local area networks (WLAN), dual-band bandpass filters (BPFs) have been proposed and exploited extensively [1–8]. Two popular methods can be classified to implement dual-band BPFs. One is realized by combining two sets of different resonators with common input and output [1, 2], which leads to a relatively large circuit size. Therefore, the other method is by utilizing a multimode resonator (MMR) with controllable resonant frequencies to design the dual-band, such as stepped impedance resonators (SIR) [3, 4], stub-loaded resonators [5, 6], and ring resonator loaded with open stubs [7, 8]. Nevertheless, the power capacity of BPF needs to be improved. In [9], resonator conducted in ground plane is proved to own a high power handling. And, recently, various kinds of defects grounded structures have been presented and find their applications in design of dual-band BPFs [10–12].

In this paper, a novel dual-band BPF based on dual-mode defected stub-loaded resonator (DSLR) is proposed. The resonant property of the DSLR cell with two fundamental resonant modes is researched. Finally, two DSLRs are cascaded to construct a dual-band BPF, and the coupling topology is studied and presented. The measured results validate the proposed design.

2. Resonant Property of DSLR

The configuration of the proposed defected stub-loaded resonator (DSLR) unit is depicted as the white part on bottom layer in Figure 1, which consists of a defected open-loop resonator and a center loaded defected stub. The DSLR is very similar to the dual-mode stub-loaded resonator (SLR) which is presented in [5] except for the ones where the proposed resonator is realized by etching a SLR on the ground plane. L_1, L_2, and H and w_1 and w_2 are indicating the defected physical lengths and widths of every sections of DSLR, respectively, and the open gap width is denoted by g. For convenience of design, $w_2 = 2w_1$ is assumed in this paper. It should be noted

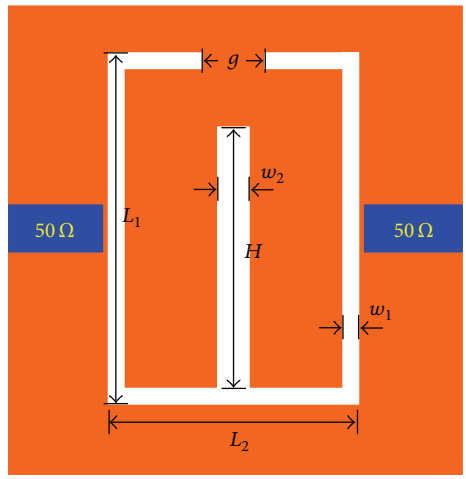

FIGURE 1: Structure of proposed DSLR unit.

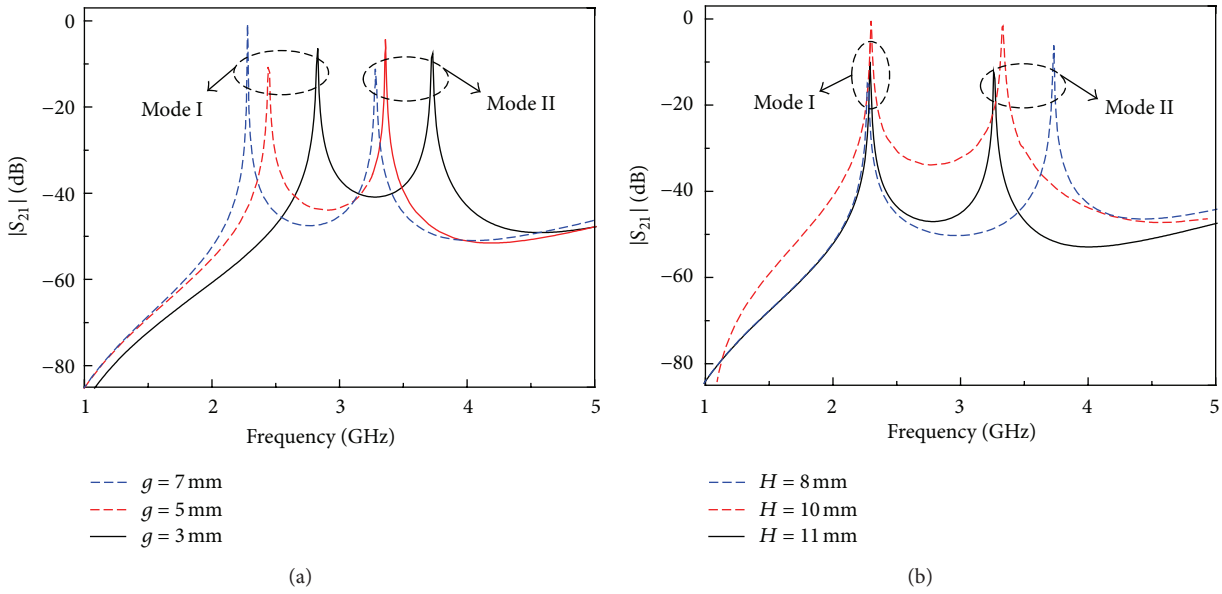

FIGURE 2: Variation of two resonant modes of DSLR with different physical length: (a) gap width (L_1 = 14 mm, L_2 = 10 mm, H = 10.3 mm, and w_1 = 0.5 mm) and (b) stub height (L_1 = 14 mm, L_2 = 10 mm, g = 5 mm, and w_1 = 0.5 mm).

here that the DSLR can be considered as several slot lines and has opposite impedance characteristics as the microstrip ones. This means a narrow w_1 results in a lower impedance, while a wide w_2 leads to a higher impedance.

To investigate the resonant property of DSLR, a full-wave EM simulator, *Ansoft HFSS* 10.0, is used to simulate the resonant cell. For providing the external excitation, a pair of 50 ohm blue microstrip feed lines on the top layer is located in both of the input and output terminal, as shown in Figure 1. The substrate adopted in this paper is FR4 material that has a relative dielectric constant of 4.5 and a thickness of 0.8 mm.

Figure 2(a) illustrates the variation of two resonant modes of DSLR, indicated by mode I and mode II, with different width g of open gap. It can be seen that the frequencies of two modes will increase as the width g of gap decreases. Meanwhile, the transmission curves about the variation of two resonant modes with loaded stub length H are depicted in Figure 2(b). From the figure, it can be observed that only mode II is varied while the first mode remains a constant when H is changing, which results in a conclusion that mode II can be controlled independently. Therefore, for giving the design specifications, it will firstly adjust the physical length of open loop to satisfy the resonant frequency of mode I. Then, tune the length of the center stub to achieve the desired resonant location of mode II.

To investigate the above-mentioned resonant characteristic of the DSLR, even and odd mode theory are used because of the symmetrical structure. Similar to the discussion in [5], the mode I (odd mode) resonant frequency can be expressed as

$$f_{\text{odd}} = \frac{(2n-1)\,c}{(4L_1 + 4L_2 - 2g)\sqrt{\varepsilon_{\text{eff}}}}, \tag{1}$$

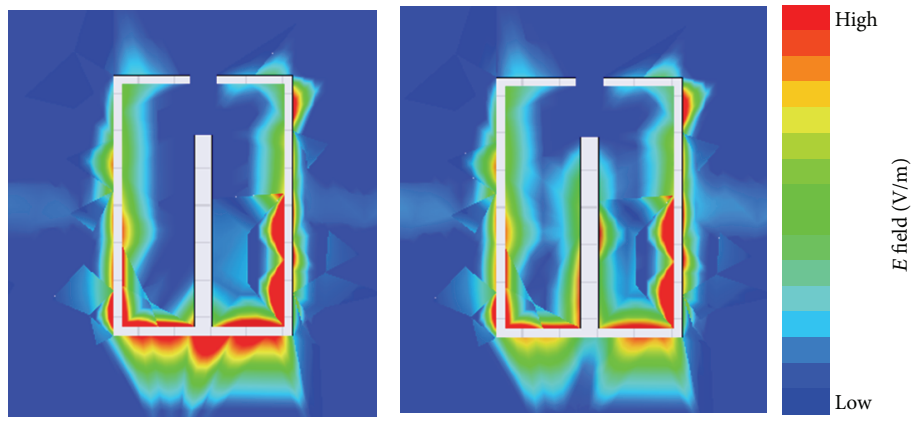

Figure 3: Simulated electric field distributions at two resonant frequencies of DSLR: (a) mode I and (b) mode II.

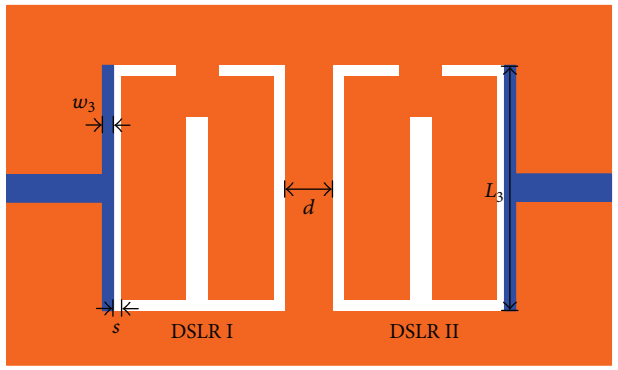

Figure 4: Configuration of the proposed DSLR dual-band filter.

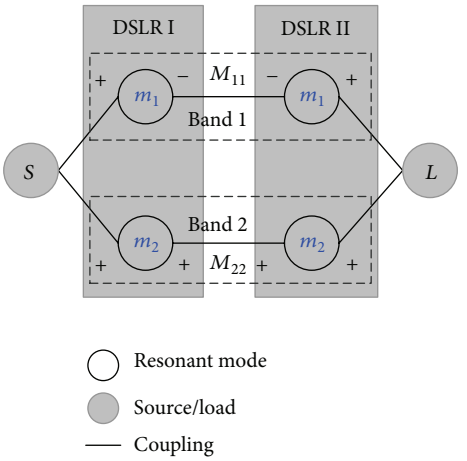

Figure 5: Coupling schematic of the designed dual-band BPF.

where $n = 1, 2, 3, \ldots$, c is the velocity of light in the free space and ε_{eff} denotes the effective dielectric constant of the slot line. Meanwhile, the mode II (even mode) resonant frequency can be calculated as

$$f_{\text{even}} = \frac{nc}{(2L_1 + 2L_2 + 2H - g)\sqrt{\varepsilon_{\text{eff}}}}. \quad (2)$$

Furthermore, the simulated electric field distributions of the dual-mode DSLR are depicted in Figure 3. It is found that the electric field at mode I is mainly distributed in open loop; the loaded stub does not work in this case. However, it is observed that a significant electric field occurs within the center stub for the second mode, which verifies the validity of Figure 2. In addition, according to the above analysis and discussions in [13], it can be easily obtained that there exists no coupling between the two resonant modes.

3. Design of Dual-Band Bandpass Filter

Based on the dual-mode DSLR, a dual-mode dual-band BPF that operates at 2.4 GHz and 3.5 GHz for WLAN and WIMAX application is implemented in this paper. To achieve two passbands with controllable bandwidth, two poles existing in each passband are needed. Therefore, as illustrated in Figure 4, two DSLRs are cascaded to obtain the dual-mode dual-band filtering response. As studied in [13], the coupling schematic of the designed dual-band BPF can be ascertained, as depicted in Figure 5. As presented, two of the first modes are coupled to form the first passband while the other two second modes are coupled to produce the second passband. For achieving the desired location of passbands, the dimensions of the DSLR that are shown in Figure 1 are finally optimized as follows: $L_1 = 14$ mm, $L_2 = 10$ mm, $H = 10.3$ mm, $g = 1.45$ mm, $w_1 = 0.5$ mm, and $w_2 = 1$ mm.

Here, a second-order Chebyshev frequency response with 0.1 dB ripple level is designed. The fractional bandwidths of two passbands are 3.3% and 2.9%, respectively. To achieve them, a certain coupling degree, including external and internal one, should be designed appropriately. The lumped circuit element values of the low-pass prototype filter are found to be $g_0 = 1$, $g_1 = 0.8431$, $g_2 = 0.622$, and $g_3 = 1.3554$. Meanwhile, the proposed dual-band filter can be equivalent to the design of two single-band filters independently, because two resonant modes of dual-mode DSLR are

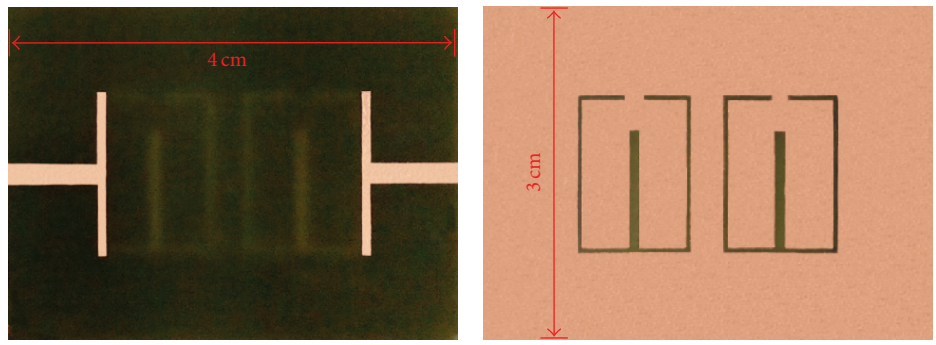

(a) (b)

Figure 6: Photographs of the fabricated DSLR dual-band filter. (a) Top view. (b) Bottom view.

decoupled [14]. Thus, the coupling coefficients and external quality factors of this filter can be calculated by [15]

$$M_1 = \frac{\text{FBW}}{\sqrt{g_1 g_2}} = 0.066, \qquad Q_{e1} = \frac{g_0 g_1}{\text{FBW}} = 17.6,$$
$$M_2 = \frac{\text{FBW}}{\sqrt{g_1 g_2}} = 0.062, \qquad Q_{e2} = \frac{g_0 g_1}{\text{FBW}} = 18.7, \tag{3}$$

where subscript 1 represents the first passband and 2 is the second passband.

When two coupled DSLRs synchronously are tuned to have a close proximity, the coupling coefficients (M_{ij}) can be obtained from the two resonant modes by using EM simulation

$$M_{ij} = \frac{f_H^2 - f_L^2}{f_H^2 + f_L^2}, \tag{4}$$

where f_H and f_L are defined to be the higher and lower of the two resonant modes. Thus, by tuning the distance d of two coupled DSLRs, two coupling coefficients will be obtained to meet the desired values, M_1 and M_2, simultaneously.

Similarly, the Q_e of the proposed filter can be extracted from the following expression:

$$Q_e = \frac{\omega_0}{\Delta\omega_{\pm 90^\circ}}, \tag{5}$$

where ω_0 and $\Delta\omega_{\pm 90^\circ}$ represent the resonant frequency and the absolute bandwidth between the $\pm 90^\circ$ points of S_{11} phase response. The EM simulator HFSS is used to extract the Q_e for two passbands. Here, a pair of T-shape microstrip feed lines, described by L_3, w_3, and s, are utilized as the input and output structure. Thus, by adjusting L_3, w_3, and s, the Q_e of two passbands can be satisfied simultaneously. Finally optimized by *Ansoft HFSS*, the rest of dimensions can be ascertained as $L_3 = 14$ mm, $w_3 = 0.5$ mm, $s = 0.43$ mm, and $d = 2.8$ mm.

4. Filter Implementation and Results

For demonstration purpose, the designed dual-band BPF using two coupled DSLRs was fabricated and its photograph with top and bottom views is shown in Figure 6. The substrate

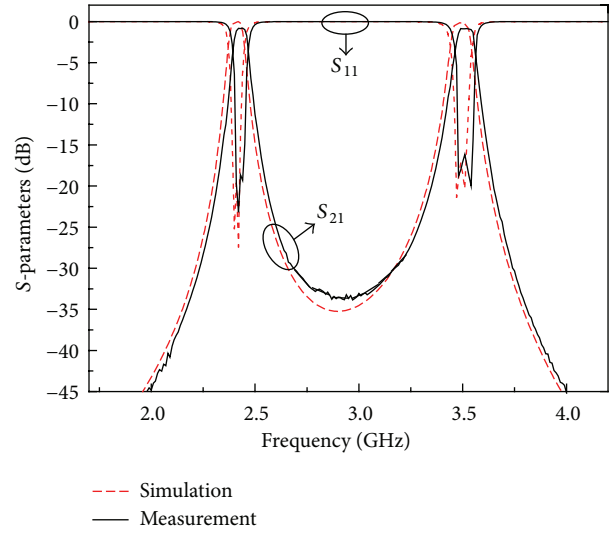

Figure 7: Simulated and measured results of the proposed DSLR dual-band BPF.

is chosen as before. The overall size of this filter except for the feed lines is $22.8 \times 14\ \text{mm}^2$ (about $0.33\lambda_g \times 0.21\lambda_g$), where λ_g is the guided wavelength at the center frequency of first passband.

Simulation and measurement were carried out using *Ansoft HFSS 10* software and Agilent's 8719ES network analyzer, respectively. The simulated and measured transmission responses are illustrated in Figure 7. The simulated results are centered at 2.40 GHz and 3.49 GHz, with 3 dB fractional bandwidths of 3.3% and 2.9%, respectively. In addition, the rejection between two passbands has reached 35 dB, which enhances the isolation of two bands. In the measurements, the two passbands are located at 2.41 GHz and 3.51 GHz, with the fractional bandwidths of 3.2% and 2.8%, respectively. Meanwhile, the measured insertion losses at center frequencies of two passbands are 0.8 dB and 0.9 dB, respectively, which are mainly attributed to the dielectric loss and radiation loss. The return losses of two bands are larger than 17 dB. Some discrepancies between simulation and measurement are caused by the inaccuracy in fabrication and implementation.

5. Conclusions

A novel dual-band BPF based on dual-mode defected stub-loaded resonator (DSLR) is proposed for WLAN and WiMAX application in this paper. The resonant property of DSLR cell with two fundamental resonant modes is researched. Finally, two DSLRs are cascaded to construct a dual-band BPF, and the coupling topology is studied and presented. The measured results validate the proposed design. The improved power-carrying capacity of the designed dual-band BPF can be used to the potential high-power application.

Conflict of Interests

The authors declare that there is no conflict of interests regarding the publication of this paper.

Acknowledgments

This work was supported by the Natural Science Foundation of Jiangxi Provincial Department of Science and Technology (no. 20122BAB211040) and the Foundation Project of East China Jiaotong University (no. 12xx02).

References

[1] C. Chen and C. Hsu, "A simple and effective method for microstrip dual-band filters design," *IEEE Microwave and Wireless Components Letters*, vol. 16, no. 5, pp. 246–248, 2006.

[2] J. X. Chen, T. Y. Yum, J. Li, and Q. Xue, "Dual-mode dual-band bandpass filter using stacked-loop structure," *IEEE Microwave and Wireless Components Letters*, vol. 16, no. 9, pp. 502–504, 2006.

[3] M. Weng, H. Wu, and Y. Su, "Compact and low loss dual-band bandpass filter using pseudo-interdigital stepped impedance resonators for WLANs," *IEEE Microwave and Wireless Components Letters*, vol. 17, no. 3, pp. 187–189, 2007.

[4] C. G. Hsu, C. Lee, and Y. Hsieh, "Tri-band bandpass filter with sharp passband skirts designed using tri-section SIRs," *IEEE Microwave and Wireless Components Letters*, vol. 18, no. 1, pp. 19–21, 2008.

[5] X. Y. Zhang, J. Chen, Q. Xue, and S. Li, "Dual-band bandpass filters using stub-loaded resonators," *IEEE Microwave and Wireless Components Letters*, vol. 17, no. 8, pp. 583–585, 2007.

[6] M. Zhou, X. Tang, and F. Xiao, "Compact dual band bandpass filter using novel E-type resonators with controllable bandwidths," *IEEE Microwave and Wireless Components Letters*, vol. 18, no. 12, pp. 779–781, 2008.

[7] S. Sun, "A dual-band bandpass filter using a single dual-mode ring resonator," *IEEE Microwave and Wireless Components Letters*, vol. 21, no. 6, pp. 298–300, 2011.

[8] S. Luo, L. Zhu, and S. Sun, "A dual-band ring-resonator bandpass filter based on two pairs of degenerate modes," *IEEE Transactions on Microwave Theory and Techniques*, vol. 58, no. 12, pp. 3427–3432, 2010.

[9] D. Ahn, J. Park, C. Kim, J. Kim, Y. Qian, and T. Itoh, "A design of the low-pass filter using the novel microstrip defected ground structure," *IEEE Transactions on Microwave Theory and Techniques*, vol. 49, no. 1, pp. 86–93, 2001.

[10] B. Wu, C.-H. Liang, Q. Li, and P.-Y. Qin, "Novel dual-band filter incorporating defected SIR and microstrip SIR," *IEEE Microwave and Wireless Components Letters*, vol. 18, no. 6, pp. 392–394, 2008.

[11] B. Wu, C. Liang, P. Qin, and Q. Li, "Compact dual-band filter using defected stepped impedance resonator," *IEEE Microwave and Wireless Components Letters*, vol. 18, no. 10, pp. 674–676, 2008.

[12] H. W. Liu, L. Shen, Z. C. Zhang, J. S. Lim, and D. Ahn, "Dual-mode dual-band bandpass filter using defected ground waveguide," *Electronics Letters*, vol. 46, no. 13, pp. 895–897, 2010.

[13] J.-S. Hong, H. Shaman, and Y.-H. Chun, "Dual-mode microstrip open-loop resonators and filters," *IEEE Transactions on Microwave Theory and Techniques*, vol. 55, no. 8, pp. 1764–1770, 2007.

[14] C. Chen, T. Huang, and R. Wu, "Design of dual- and triple-passband filters using alternately cascaded multiband resonators," *IEEE Transactions on Microwave Theory and Techniques*, vol. 54, no. 9, pp. 3550–3558, 2006.

[15] J.-S. Hong and M.-J. Lancaster, *Microwave Filter for RF/Microwave Application*, John Wiley & Sons, New York, NY, USA, 2001.